

**DEVELOPMENT OF A NEW SUBSURFACE STRAIN AND DISPLACEMENT
SENSOR TO BE USED IN SOIL**

Vanessa Andrews, University of Tulsa
Host Institution: University of California, Davis
REU Advisor: Dr. Bruce L. Kutter
PhD Mentor: Ray-Ching Chou

1. ABSTRACT

Researchers at UC Davis are developing methods for using electrical resistivity concepts to measure strain and displacement in geotechnical centrifuge tests. One application is in printing very small electrodes on a flexible plastic sheet, in order to measure shear strain caused by waves with very steep acceleration pulses. Because of the high initial fabrication costs of these sensors, it is desirable to test a scale model of the sensor in order to determine feasibility and optimize the sensor geometry. A second application is in measuring the displacement of the foundation in a centrifuge test of the Bay Area Rapid Transit (BART) tube. While size constrictions are less critical in this application, the principles are still relatively untested, so a model is used to determine feasibility and optimum geometry.

Scale models of the sensors to be used in each of these applications were constructed. While the sensors are designed to be used in soil, the models were tested and calibrated in water so that displacement and strain could be easily performed and measured. Both sensors utilized a configuration similar to a Wheatstone bridge, so that the voltage across two of the electrodes changed as the sensor was deformed. In both cases, the relationship between voltage and deformation was approximately linear, and the repeatability between tests was good. Effects of various factors, including frequency, time, and sensor size, were tested, and their consequences noted; however, the effect of any of these factors was far less significant than the effect of the relevant factors (angle/distance), suggesting the model's feasibility as a strain sensor. The next step is to develop specific technical specifications for the sensors, and then calibrate the sensors.

2. INTRODUCTION

This paper discusses two related projects, both of which involve developing sensors that use resistivity concepts to measure displacement in soil. The first project involves developing an angular displacement sensor to be used to measure the rise time of very steep fronts for shear waves that have been observed in centrifuge model tests, while the second involves developing a linear displacement sensor for use in a project involving seismic retrofitting of the underwater tube of the Bay Area Rapid Transit (BART) system.

2.1. De-Liquefaction Shock Waves

On a seismogram, the largest amplitude spikes typically occur shortly after the first break, when the ground motion is strongest. However, in areas of liquefaction, large amplitude spikes are sometimes seen late in the seismic record, after most of the ground motion has stopped. These amplitude spikes are believed to be caused by shock waves formed by the temporary solidification of soil caused by dilatancy at large shear strains, or "de-liquefaction" (Kutter and Wilson, 1999).

Kutter and Wilson (1999) describe the process by which geotechnical centrifuge tests can be used to model de-liquefaction shock-wave formation. The observed shock waves are

slow-moving but spatially sharp, with a wavelength of about 0.1 m. The acceleration pulse is very steep, appearing to increase from 0.1 to 0.34 g in less than 0.5 m (prototype scale). At the centrifuge model scale, the length of the wave front is on the order of a couple millimeters. The resolution of the acceleration curve, however, is limited by the size of the accelerometers that have been used in the past. More accurate definition of the wavefront will require sensors that can resolve spatial distributions of accelerations or strains with resolution of about 1 mm. A concept is being developed to make miniature soil strain sensors at the 1 mm scale. The sensors would consist of electrodes printed on a flexible plastic sheet that can be buried in the soil.

As is common in various types of strain sensors, these sensors will make use of a Wheatstone bridge (Fig. 1). Simple circuit math shows that, for any Wheatstone bridge,

$$V_o/V_i = R_4/(R_3+R_4) - R_2/(R_1+R_2) \quad (1)$$

where V_o and V_i are in volts and the resistances are in Ohms.

The resistances between electrodes are related to the distances between electrodes, thus relative movement of buried electrodes will cause resistances R_1 to R_4 to change and produce an output signal, V_o , which can be used to determine shear strain to be estimated from the measured voltage across the circuit. This methodology will be further discussed in Section 3.

Dr. Bruce Kutter has submitted a proposal to the USGS requesting funding in order to perform centrifuge tests on this subject at the NEES Center for Geotechnical Modeling, located at UC Davis. If the proposal is approved, a test of de-liquefaction shock-wave formation using millimeter-scale sensors will be performed in approximately February 2008.

Initial fabrication costs for these sensors, however, are fairly high, and the principles of operation are new and untested. Therefore, it is desirable to test a scale model of the sensor to determine accuracy and optimal electrode configuration. This model will be referred to as an angular displacement sensor in Section 3.

2.2. Seismic Retrofitting of the BART Transbay Tube

BART is a public transportation system, similar to a subway, that services much of the San Francisco Bay area. The rail system includes a 3.6 mile, 24' high by 48' wide tube that travels beneath the San Francisco Bay. The tube is valued at \$176 million. BART is interested in seismically retrofitting the tube, and has contracted with several organizations, including Fugro West Inc., to propose a seismic retrofit design.

Fugro West has hypothesized that at least one section of the tunnel, known as Zone 5, is already able to adequately withstand an earthquake, and does not need seismic retrofitting. The team, led by Thaleia Trarasarou, is in the process of designing multiple tests of this hypothesis, including a centrifuge test.

One of the goals of the centrifuge test is to measure relative displacement between the top and bottom of the foundation. Measuring relative distances at depth, however, is an inherently difficult problem, because with conventional displacement sensors it is difficult to measure the displacement without disturbing the soil. Electrical resistivity concepts may also be useful in this case. It is hoped that parallel plate sensors placed at the top and bottom of the foundation, referred to as linear displacement sensors in Section 4, will help solve this problem.

3. ANGULAR DISPLACEMENT SENSOR: PROCEDURE AND RESULTS

3.1. Model design and theoretical voltages

The model consists of four brass electrodes of 1-cm diameter glued on each side of two pieces of plastic, which are hinged using insulating tape (Fig. 2a). The electrodes are configured in a square so that, when the model is undeformed, the distance, and thus the resistance, should be the same between each pair of adjacent electrodes, allowing the construction of a circuit similar to a Wheatstone bridge (Fig. 1). The wire is soldered onto the face of the electrode that is against the plastic, so that the exposed face is uniform brass.

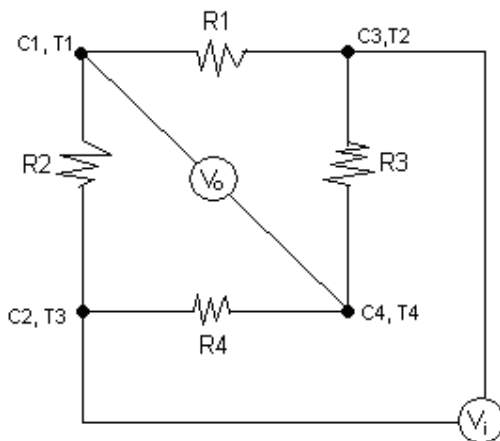


Figure 1. Circuit diagram

While the final sensor is to be used in soil, the model is tested in water, so that angular displacement may be easily adjusted and measured. The model is submerged in saltwater with a conductivity of between 1.8 and 2.0 mS/cm, and secured in place using a plastic clamp, as shown in Fig. 2b. The angle is adjusted manually. A protractor at the bottom of the container allows for easy angle measurement.

A signal generator introduces AC current across C2 – T3 and C3 – T2. An oscilloscope is used to measure the input voltage. Voltage is then measured across C1 – T1 and C4 – T4 using a voltmeter. Electrode pairs indicated with a hyphen are short-circuited.

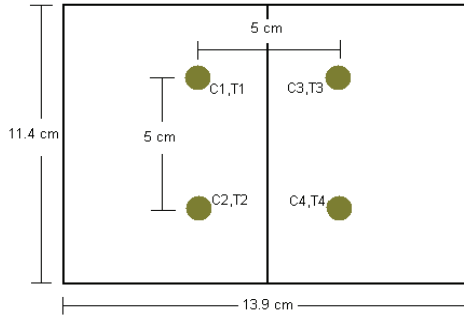


Figure 2a. Sensor diagram

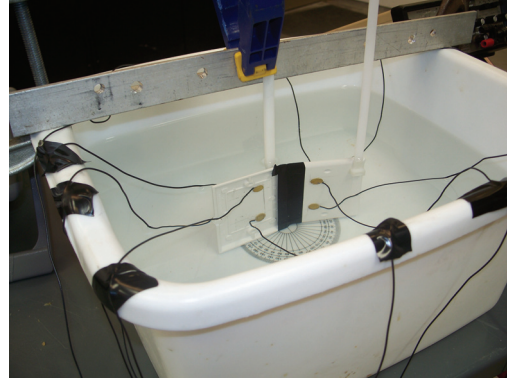


Figure 2b. Test setup

The model uses a center-to-center spacing of 5 cm between adjacent electrodes. The distance traveled by the current between either T1 and T2 or T3 and T4 is approximately 5 cm, regardless of the angle. The law of cosines shows that, when the plastic is bent at the hinge, the distance d between either C_1 and C_2 or C_3 and C_4 is approximated by the formula,

$$d = 2 * (d/2)^2 * (1 - \cos(\alpha)) \quad (2)$$

where α is the angle between the two plates and can vary from 0 to 180 degrees. The resistances are approximated by the formula,

$$R_1 = R_4 = 2 * (1 - a/d_s) * \rho / (2\pi a) \quad (3)$$

and

$$R_2 = R_3 = 2 * (1 - a/d) * \rho / (2\pi a) \quad (4)$$

where ρ is the resistivity in ohm-cm of the material between the electrodes and a is the radius in cm of the sphere with equivalent surface area (Mazbich, 1965). The factor of 2 is necessary to account for the doubled resistance resulting from the electrodes being fixed to an insulating material on one side. The electrodes are thin enough that their thickness may be ignored, so the exposed surface area is equal to the area of a circle with radius 0.5 cm. It is easily shown that the electrode has equivalent surface area to a sphere of $a = 0.25$ cm.

Since $R_1 = R_4$ and $R_2 = R_3$, Eq. 1 can be replaced by

$$V_o/V_i = (R_1 - R_2) / (R_1 + R_2) \quad (5)$$

$$= (2 * (1 - a/d_s) * \rho / (2\pi a) - 2 * (1 - a/d) * \rho / (2\pi a)) / (2 * (1 - a/d_s) * \rho / (2\pi a) + 2 * (1 - a/d) * \rho / (2\pi a))$$

Simplifying this equation yields,

$$V_o/V_i = (3.8 + (4 - 1/(12.5(1 - \cos(\alpha))))^{1/2}) / (3.8 - (4 - 1/(12.5(1 - \cos(\alpha))))^{1/2}) \quad (6)$$

It is now clear that resistivity should not affect the voltage. A plot of theoretical voltage versus angle is shown in Fig. 3. Only angles of deformation from 0 to 40 degrees are considered ($0^\circ < (\theta = 180^\circ - \alpha) < 40^\circ$), as this already exceeds realistic amounts of deformation in soils, and at higher angles it is difficult to accurately calculate strain.

For small angles of strain, strain can be estimated by the formula,

$$\gamma = \sin(180-\alpha)/2 \tag{7}$$

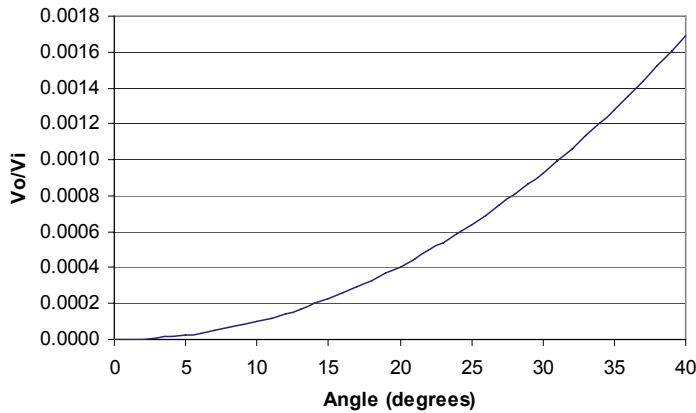


Figure 3. V_o/V_i versus angle (theoretical)

Fig.4 shows a plot of strain versus voltage. While voltage was previously the dependent variable, it is now plotted as the independent variable, as the goal is to determine strain from voltage.

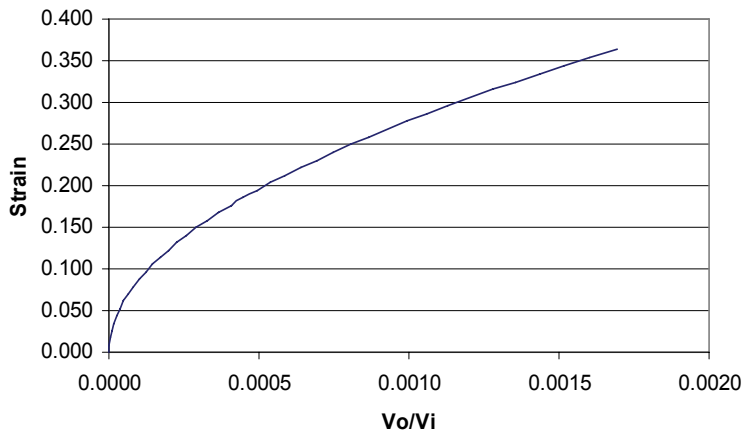


Figure 4. Strain versus V_o/V_i (theoretical)

3.2 Results

3.2.1 Feasibility of Proposed Sensor Configuration

While the output voltage should ideally depend only on input voltage and angle, it is desirable to check dependence on other factors, in order to determine the degree of any

electrode effects.

Observation showed that the output voltage was affected by moving the wires within the saltwater, so steps were taken to secure the wires.

Fig. 5 shows the results of a test done while maintaining constant frequency ($f = 10 \text{ kHz}$) and angle ($\theta = 30^\circ$) and varying the input voltage. While V_o/V_i should ideally remain constant, the figure shows a small increase in V_o/V_i with increasing V_i . However, a single test would be performed at a constant input voltage, so while the results of this test demonstrate an electrode effect, this effect is unlikely to impact the accuracy of testing.

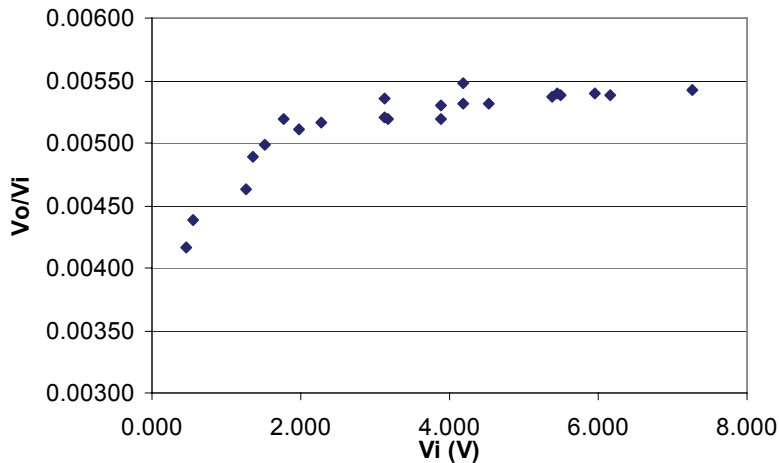


Figure 5. V_o/V_i versus V_i ($f = 10 \text{ kHz}$, $\theta=30^\circ$)

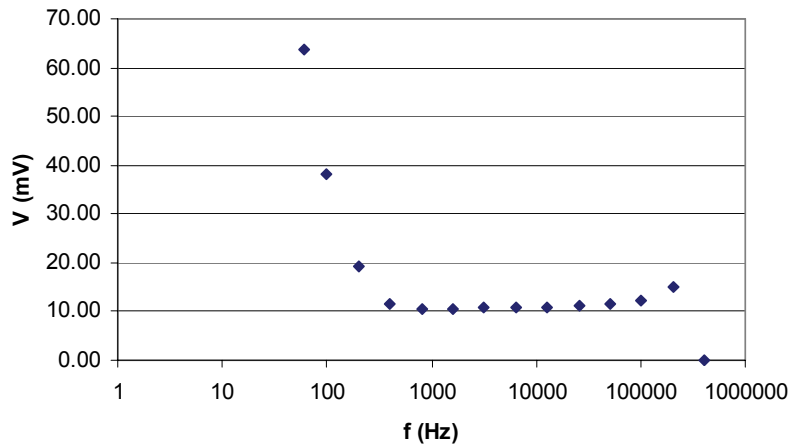


Figure 6. Voltage versus frequency ($V_i = 3V$, $\theta=30^\circ$)

While voltage increases with frequency for mid-range frequencies, it will decrease sharply at frequencies higher than approximately 310 kHz and will increase with decreasing frequencies for frequencies below approximately 500 Hz. A graph of voltage versus frequency is shown in Fig. 6.

In Fig. 7, one can see the time dependency of voltage at various frequencies. Input voltage ($V_i = 3V$) and angle ($\theta = 30^\circ$) remain constant. Note that while the minimum and maximum values of voltage changes between graphs, the range remains the same, so that the time dependency may be seen visually. While it is interesting to note that the voltage may either increase or decrease with time, depending on frequency, the more relevant information is that the voltages are most stable for mid-range frequencies.

To test the dependence of voltage on angle, a frequency of 10 kHz was chosen, due to voltage stability at that frequency and to the limitations of equipment that will be used in later testing. For small angles ($\theta < 40^\circ$), voltage increases linearly with frequency. Four trials were performed with the signal generator continuously on, and four were performed with the signal generator turned off and on between each reading, to determine if the electrodes were subject to significant corrosion induced by the current, which might cause a change in electrode resistance and an erroneous output signal. Fig. 8 shows all eight trials on the same plot; it is evident that the duration of excitation does not cause any significant difference.

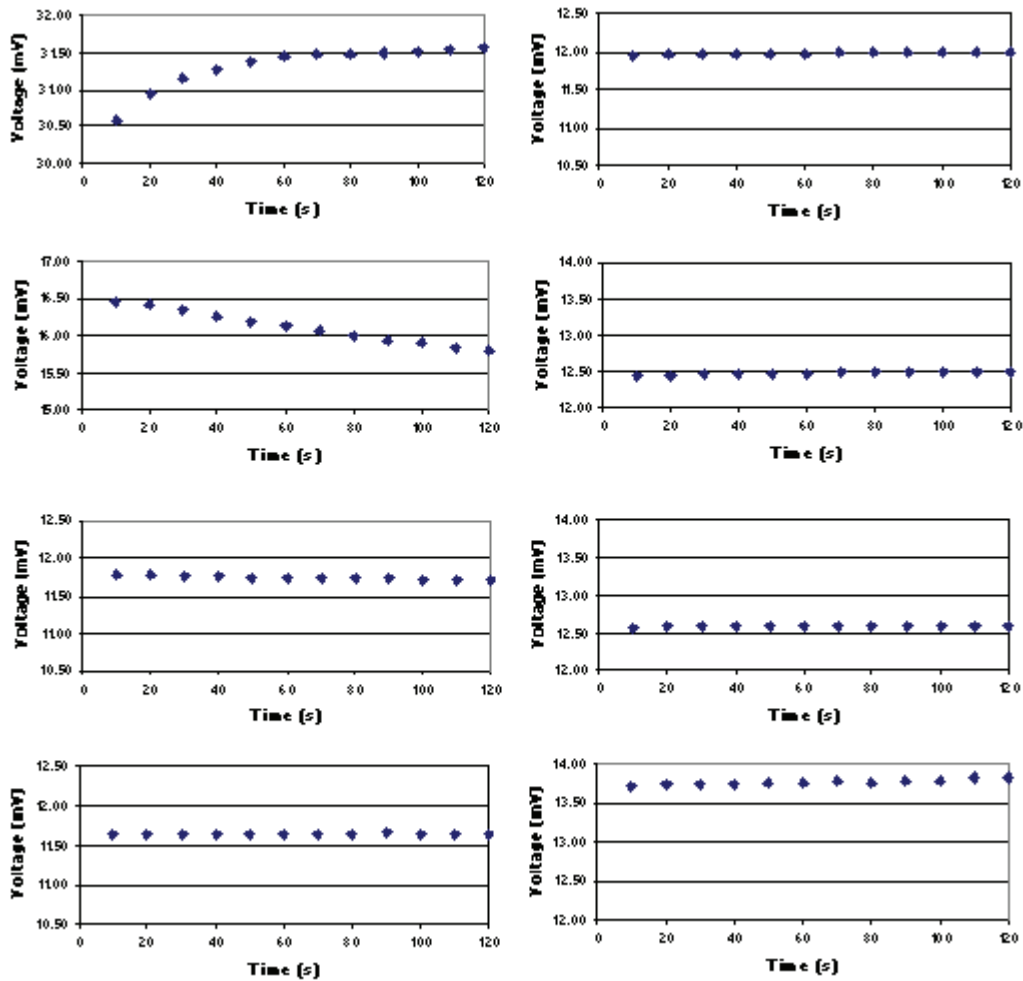


Figure 7. Voltage vs. time for various frequencies ($V_i = 3V$, $\theta = 30^\circ$)

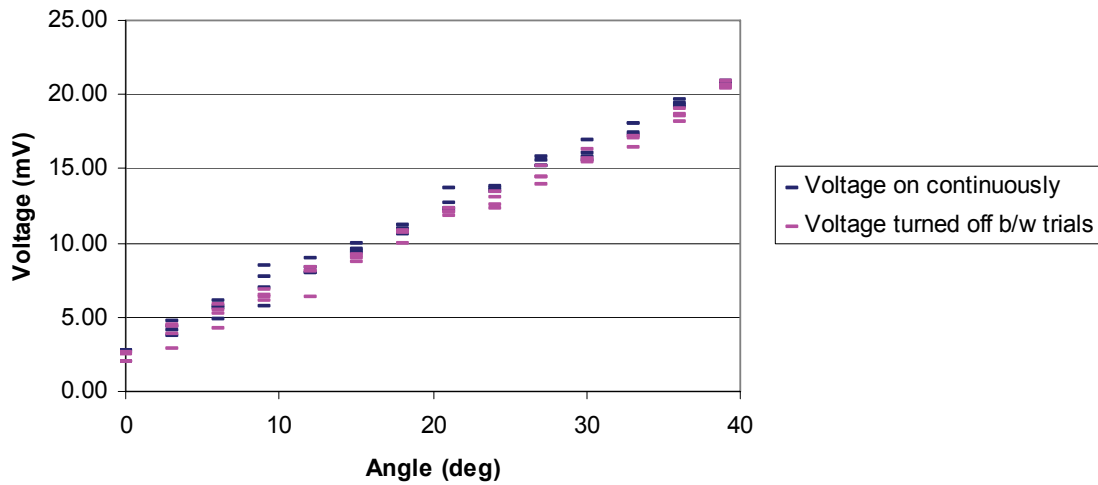


Figure 8. Voltage v. Angle ($f = 10$ kHz, $V_i = 3V$)

The above evidence is sufficient to show that angle, and therefore strain, may be adequately determined from the proposed sensor configuration, as will be discussed further in Section 5. The following section integrates theory and experimental data to refine the parameters of the proposed circuit.

3.2.2. Optimization of Sensor Parameters

First, the optimum value of d_s/a is discussed, where a is the radius area of a sphere with equivalent surface area to the electrode and d_s is the distance between electrodes on an undeformed sheet. Refer to Eq. 3. This equation applies only if there is adequate distance between the electrodes; here, we will assume that $d \geq a$. An examination of this equation shows that R increases asymptotically from 0 to $(2\pi a)^{-1}$. It is clear that the sensitivity of R to d_s is lower at values of d_s that are much larger than a , and thus the voltage sensitivity would also be lower. While the voltage sensitivity is greatest at values of d_s close to a , the applicability of the theory at small values of d_s has not been determined, so it is also undesirable to choose a small value of d_s . While future studies could further refine the parameters, this equation is sufficient to show that the value of 20 chosen for d_s/a in the model has adequate sensitivity of resistance to distance.

The significance of edge effects would require 3-dimensional numerical modeling to determine theoretically, which is beyond the scope of this project. Instead, the significance is explored experimentally, by creating a sensor the same electrode spacing but greater edge distance (edge distance = 5.2 cm). A graph of voltage versus angle is shown in Fig. 9. Note that the voltages are lower (and thus closer to the theoretically predicted voltages, which assumed an infinite edge distance), but that the linearity and consistency are similar. Since the sensor will need to be calibrated regardless of correlation with theory, this test suggests that edge size is not a significant factor in the sensor's accuracy after calibration.

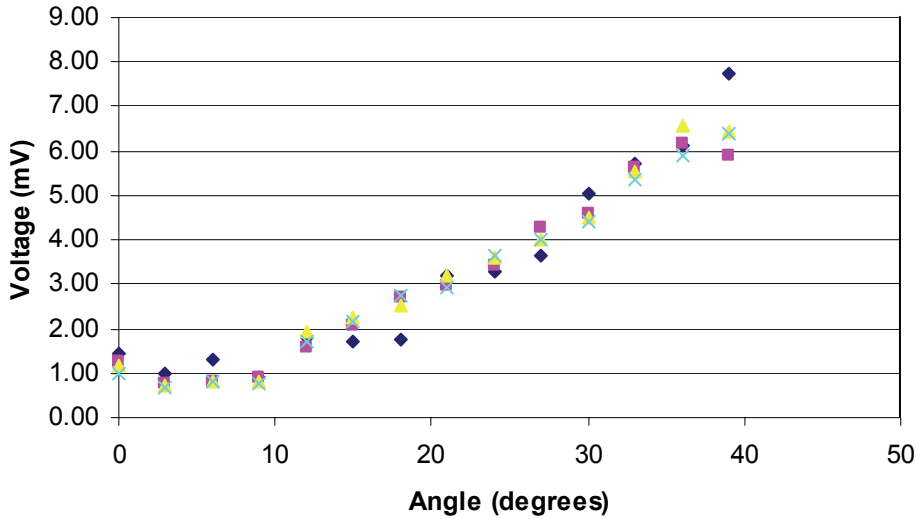


Figure 9: Voltage v. Angle (larger sensor)

4. LINEAR DISPLACEMENT SENSOR: PROCEDURE AND RESULTS

4.1. Model design and theoretical voltages

This model uses two plates with two electrodes each, as shown in Fig. 10a. They are also configured similarly to a Wheatstone bridge (Fig. 10b), but with only one electrode composing each node of the bridge, rather than two as in the previous model. The plates were submerged in saltwater, and were initially parallel, with the electrodes facing each other (Fig. 11).

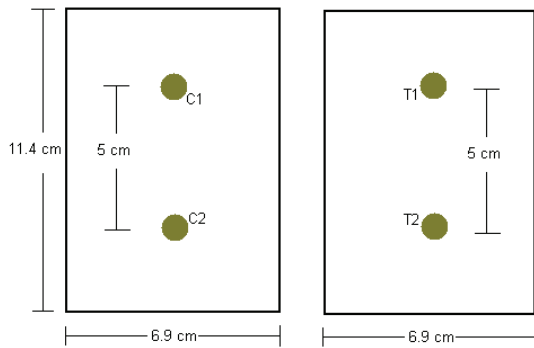


Figure 10a: Sensor design

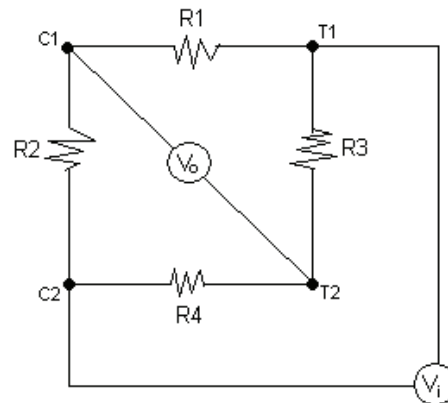


Figure 10b: Circuit diagram

Theoretical voltages are calculated similarly for this model as for the first one. The primary difference is that distances are measured directly instead of calculated from the angle. This change allows the simplification of Eq. 5 to,

$$V_o/V_i = (0.2*d-1)/(7.8*d-1) \tag{8}$$

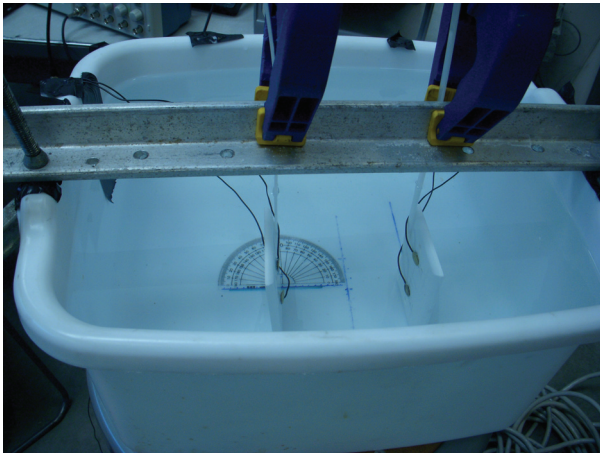


Figure 11: Test setup

4.2. Results

In the first test, the plates remain parallel, while one of the plates is moved toward and away from the other plate. As anticipated theoretically, the amplitude of the output voltage is very high when the plates are close together, it decreases to near 0 as the plates move further apart, and then increases again (Fig. 12a). A close-up of the section from 3.5 to 10 cm allows the turning point to be seen more clearly (Fig. 12b).

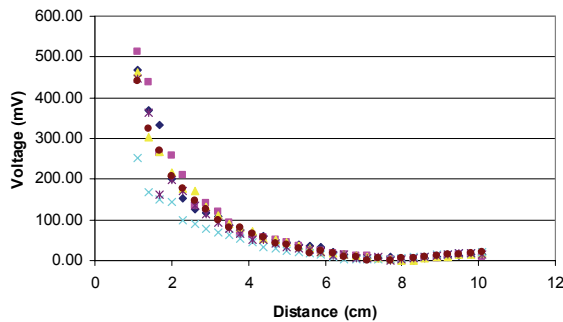


Figure 12a. Voltage v. Distance (1.1-10 cm, $V_i = 3V$, $f = 10$ kHz)

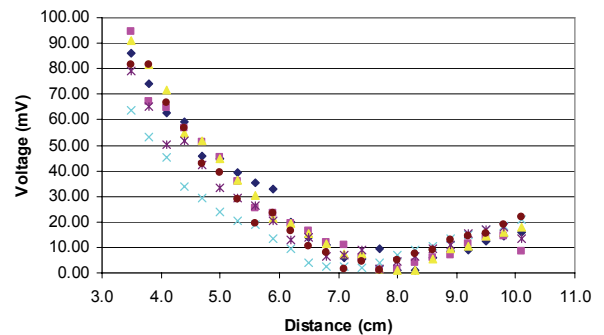


Figure 12b. Voltage v. Distance (3.5-10 cm, $V_i = 3V$, $f = 10$ kHz)

In the second test, the plates remain 5 cm apart in the x-direction, while one plate is moved to one side (Fig. 13a). In the third test, the plates again remain 5 cm apart in the x-direction, and one plate is moved vertically (Fig. 13b). In both tests 2 and 3, the total distance is calculated using the Pythagorean Theorem. Fig. 14 shows all three of these tests, along with the theoretical voltages. Because only the magnitude of the voltage is measured, not the sign, the absolute values of the theoretical voltages are plotted. Note both that the fit between theoretical and measured voltages is quite good, considering the simplicity of the model used to calculate them, and that the voltage is reasonably independent of the direction of motion.

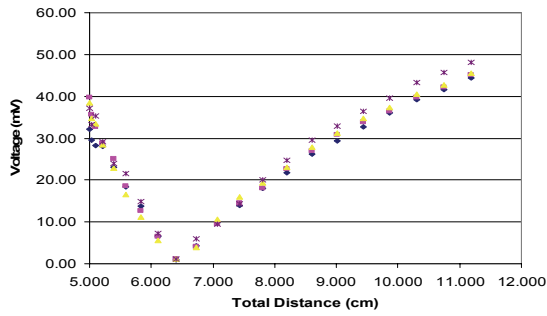


Figure 13a. Voltage v. Distance (y-dir.)

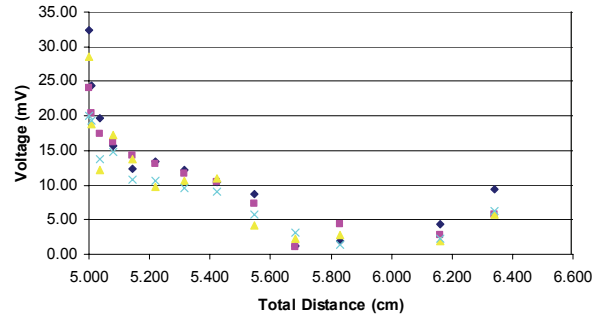


Figure 13b. Voltage v. Distance (z-dir.)

The effect of rotations around each axis were also tested (Fig. 15), with the center-to-center spacing between the sensors kept constant.

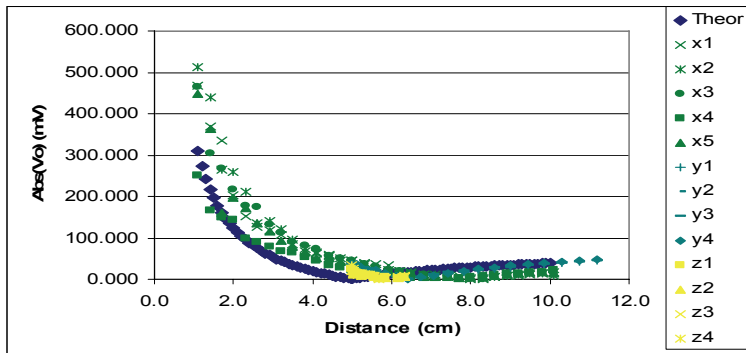


Figure 14. Voltage vs. Distance (all directions and theoretical)

5. DISCUSSION AND FUTURE TESTING

In order to serve as an accurate strain or displacement sensor, the sensor must be far more sensitive to the relevant factors (angle and/or distance) than to any other factor. Sensitivities to each factor were calculated by dividing the absolute value of the change in voltage by the change in the relevant factor over a certain range. Table 1 shows the values of sensitivity to angle (S_θ) from 0 to 39 degrees, sensitivity to frequency (S_f) from 1 to 100 kHz, and sensitivities to time ($S_{t,f}$) at various frequencies from 50 Hz to 100 kHz. Above about 100 kHz, voltages become unstable, so there is no clear relationship between voltage and time.

Note that the effect of changing the angle by 1° produces roughly the same output as changing the frequency by a factor of 10. Since the frequency would be kept constant during the centrifuge tests, with some minor variations, the effect of frequency appears insignificant.

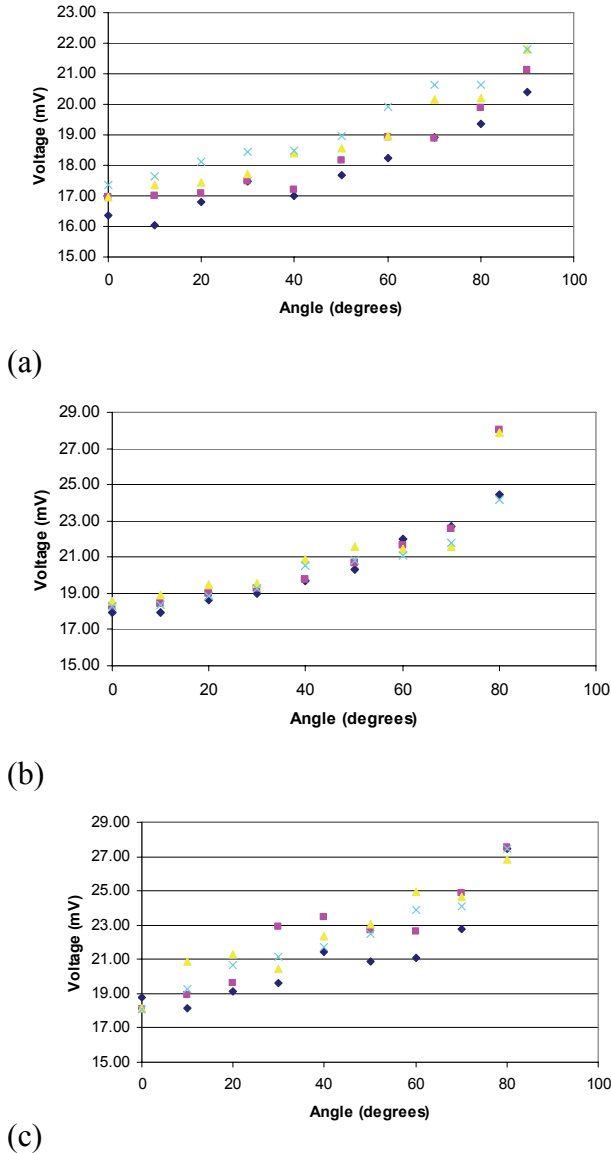


Fig. 15: Rotations around the x- (a), y- (b), and z- (c) axes.

Table 1 also indicates the importance of choosing a proper frequency. While at mid-range frequencies the effect of time is fairly insignificant, given the short time that the signal generator would be on, time is a very significant factor at low frequencies.

Table 2 shows the sensitivities for each of the six degrees of freedom (rotations around the x-, y-, and z-axes, and motions in the x-, y-, and z-directions, calculated from 0 to 80 degrees for rotations, from 1.1 to 10.1 cm for S_x , from 0 to 10 cm for S_y , and from 0 to 3.9 cm for S_z . S_x and S_y were calculated by taking a weighted average of the sensitivities of the section in which the voltage decreased and the section in which the voltage increased. S_f is again calculated from 1 to 100 kHz.

Table 1: Sensitivities of Sensor 1 to various parameters

Parameter	Units	Value
S_{θ}	mV/deg	0.455
S_f	mV/log(Hz)	0.471
$S_{t, 50 \text{ Hz}}$	mV/min	0.540
$S_{t, 100 \text{ Hz}}$	mV/min	0.366
$S_{t, 500 \text{ Hz}}$	mV/min	0.033
$S_{t, 1 \text{ kHz}}$	mV/min	0.011
$S_{t, 5 \text{ kHz}}$	mV/min	0.027
$S_{t, 10 \text{ kHz}}$	mV/min	0.022
$S_{t, 50 \text{ kHz}}$	mV/min	0.011
$S_{t, 100 \text{ kHz}}$	mV/min	0.054

While there is much more frequency dependency with this sensor than with the previous sensor, it is still not enough to be significant if the frequency remains relatively constant. The most important information is that the sensor is sensitive to all six degrees of freedom, indicating that the sensor's motion would have to be restricted to certain

Table 2. Sensitivities of Sensor 2 to various parameters

Parameter	Units	Value
S_{θ_x}	mV/deg	0.050
S_{θ_y}	mV/deg	0.075
S_{θ_z}	mV/deg	0.117
S_x	mV/cm	8.938
S_y	mV/cm	7.264
S_z	mV/cm	9.011
S_f	mV/log(Hz)	3.713

directions and/or a grid of sensors would have to be used and their output voltage compared, in order to determine the direction of motion.

Both sensors are far more sensitive to angle and/or distance than to any other tested parameter, indicating that they would be feasible strain sensors. In each test, the next step is to use the guidelines presented in this paper to develop specific technical specifications, and then to build and calibrate the prototype sensors.

References

Isbell, William M. (2005). *Shock Waves: Measuring the Dynamic Response of Materials* (Imperial College Press, London).

B.L. Kutter, "Dynamic Centrifuge Modeling of Geotechnical Structures", Transportation Research Record 1336, TRB, National Research Council, pp. 24-30, Washington, D.C., 1992.

Kutter, B. L., and Wilson, D. W. (1999). "De-liquefaction shock waves." *Proc., 7th U.S.–Japan Workshop on Earthquake Resistant Design of Lifeline Facilities and Countermeasures Against Soil Liquefaction*, Seattle, 295–310.

Lee, Jong Sub (2003). "High Resolution Geophysical Techniques for Small-Scale Soil Model Testing." PhD Dissertation. Georgia Institute of Technology, Atlanta, GA.

Mazbich, B.I. (1966). "Measurement of the specific electrical resistance in the functioning lung of man and the dog." Translated from *Byulleten' Eksperimental'noi Biologii i Meditsiny*, Vol. 61, No. 2, pp. 120-123.